Chapter 4

Development process for synchronous filter

4.1 Introduction

One of the main objectives for the development of a synchronous filter for gear vibration is to reduce the amount of gear vibration data that needs to be stored in the data acquisition system in order to calculate the time-domain average (synchronous average) of the gear vibration data. This space saving can bring us a step closer to the development of a truly online gear condition monitoring system that utilises time domain averaging to enhance the diagnostic capability. The reduction in the amount of data that needs to be stored in the data acquisition system allows for data acquisition and analysis to be executed simultaneously. In Chapter 3 the theory of MLP, RBF networks and SVMs in the light of this work was presented. Their suitability for use in a time domain averaging task was also assessed. In this chapter, two models for synchronous filtering of gear vibration are presented. The proposed models are implemented using each of the three mathematical formulations and their performances are compared. A detailed explanation of the experimental set-up is also presented.

4.2 ANNs and SVMs synchronous filtering model

In neural networks input space reduction is achieved by transforming the input data space into a lower dimensional space or trimming off the redundant features in the input space. Transformation of the input space to lower dimensional space is achieved by using a procedure like Principal Component Analysis (PCA) (Bishop, 1995). Engineering judgement and procedures like Automatic Relevance Determination (ARD) (MacKay, 1994; Neal, 1996; Neal, 1998) are used to prune the input space. Mdlazi et al. (2003) compared the performance of ARD to PCA focusing on the practical implementation issues of the two input-selection schemes using practical vibration examples.In this work, the interest is in the time domain representation of the gear vibration data and moreover, it is undesirable to lose any of the underlying dynamics within the input space, which could be the case when the input space is pruned.

The requirement for time domain representation of the gear vibration data and input space reduction results in the requirement of efficiently mapping the input space (rotation synchronised gear vibration signal) to the output space (time domain average of the vibration signal) using less data than would otherwise be used in the direct time-domain averaging procedure.

ANNs and SVMs are suitable in such applications because of their non-linear mapping and generalisation capabilities (Bishop, 1995; Gunn, 1998). In this paragraph the developed filtering technique is described. The main idea is to simulate direct TDA using artificial intelligence, in this case ANNs and SVMs. This approach has the potential of reducing the amount of vibration data that is required to calculate the TDA by direct averaging if the ANNs and SVMs can successfully map a fraction of the input pace to the output (TDA calculated by direct averaging of all the input data) as shown in Chapter 3. The performance of this filtering approach will therefore depend the non-linear mapping and generalisation capabilities of ANNs and SVMs. This filtering concept operates in two stages as shown in the block diagram in Figure 4.1.

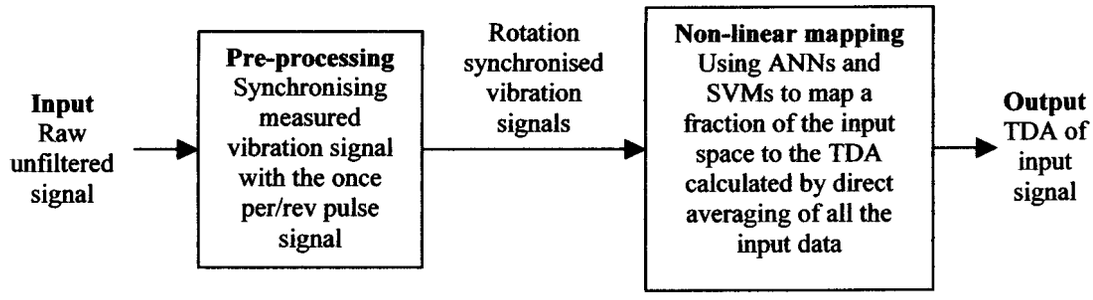

Figure 4.1 ANNs and SVMs base filtering concept.

More detail the different stages of this filtering technique are discussed later on in this chapter. Before much more is said about the data it is appropriate to describe the experimental set-up.

4.2.1 Experimental set-up

The data used in this study was obtained from the accelerated gear life test rig developed by Stander and Heyns (2002[a]) for their work on condition monitoring of gearboxes under fluctuating load conditions.

This experimental set-up consists of three Flender Himmel Motor helical gearboxes, driven by a 5.5 kW three-phase four pole WEG squirrel cage electric motor. A 5.5 kVA Mecc alte spa three-phase alternator was used for applying the load. The gear test rig was designed to conduct accelerated gear life tests on the Flender E20A gearbox under varying load conditions. Two additional Flender E60A gearboxes were incorporated in the design in order to increase the torque applied to the small Flender E20A gearbox. The rated load of the gears in the Flender E20A gearbox was 20 Nm. The Direct current (DC) fields of the alternator were powered by an external DC supply in order to control the load that was applied to the gears. A Hengstler R176T01 1024ED 4A20KF shaft encoder, which produced 1024 pulses, and 1 pulse per revolution in the form of an analog push-pull signal was used to measure the shaft speed. The reference point for synchronous averaging is measured as a single pulse from the shaft encoder. Acceleration measurements were taken in the vertical direction with a 5 V/g PCB integrated circuit piezoelectric industrial accelerometer and a Siglab model 20-42 signal analyser (Stander and Heyns, 2002[a]). The accelerated gear life test rig is shown in Figure 4.2.

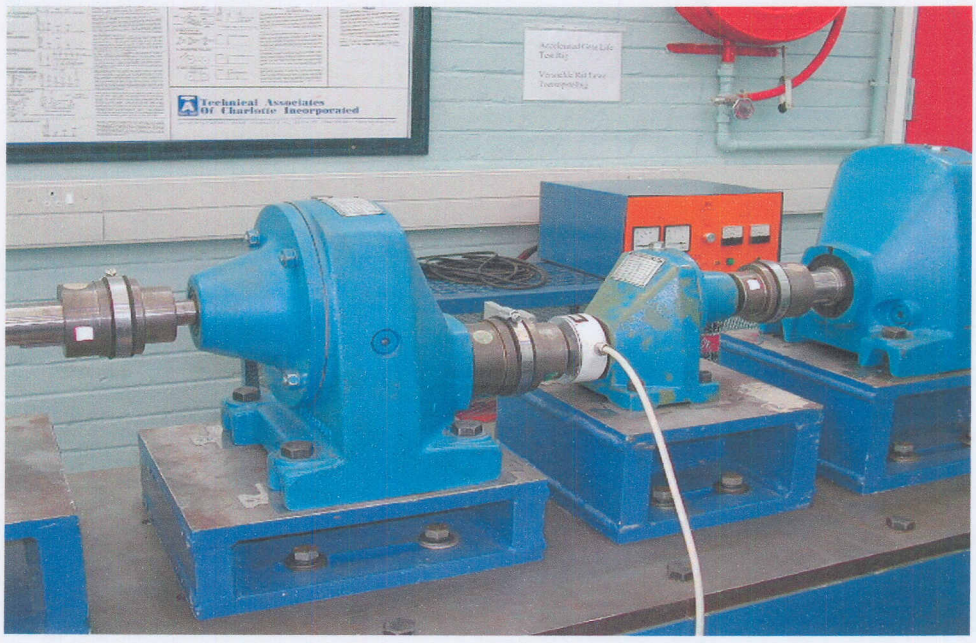

Figure 4.2 Accelerated gear life test rig.

The gears used in this experiment were manufactured in accordance with DIN3961, Quality 3. The gear specifications are given in Table 4.1 (Davel, 2003).

Table 4.1 Gear Specifications for gears used in accelerated gear life test rig.

Description	**Specification**
Helix angle at reference circle	30^{o}
Number of teeth (Pinion)	22
Number of teeth (Gear)	43
Nominal Module	1.250 mm
Base circle radius (Pinion)	14.64 mm
Base circle radius (Gear)	28.61 mm
Tip radius (Pinion)	17.55 mm
Tip radius (Gear)	0.331 mm

A typical signal obtained from the accelerometer is given in Figure 4.3 (a). This signal is synchronised with the pulse signal given in Figure 4.3 (b) in order to isolate the vibration that is produced by each gear rotation.

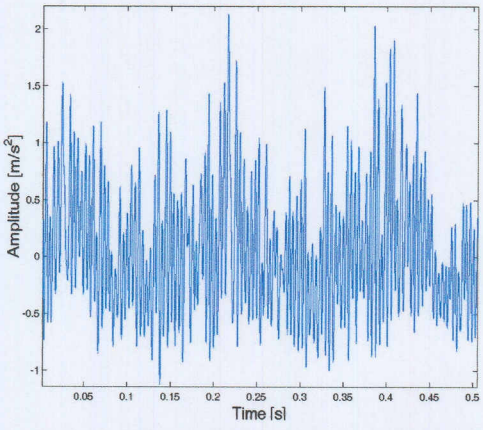

Figure 4.3 (a) Measured acceleration signal over 0.5 seconds.

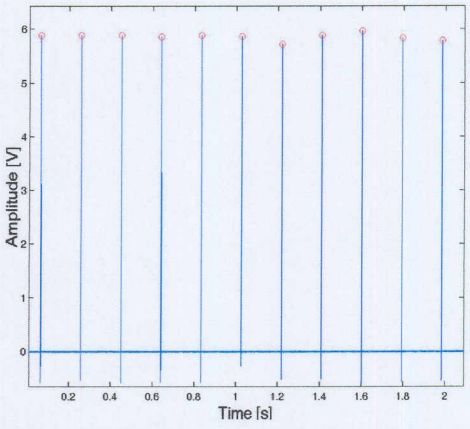

Figure 4.3 (b) One pulse per/rev shaft encoder signal for synchronising the gear vibration.

In order to assess the performance of the developed synchronous filter under both constant and varying load conditions, the measurements were also taken under different load conditions over the entire life of a gear. The load on the gearbox was applied by changing the current supplied to the alternator. The different loading conditions are given in Table 4.2.

Table 4.2 Experimental load conditions

Type of loading	Accelerated life test	Constant load	Sine function	Square function	Random function
Frequency [Hz]	0.0	0.0	0.5	0.3	2.0-5.12
Amplitude [V]	0.0	0.0	2.0	2.0	2.0
Offset [V]	5.0	3.0	3.0	3.0	3.0

4.2.2 Data processing

The acceleration data obtained from the gear test rig is passed through an eighth order low pass Butterworth filter with a cut-off frequency of 300 Hz. The acceleration signal is sampled at 51.2 kHz to ensure a true data representation. The filtered acceleration signal is synchronised with the pulse signal. The signals obtained after synchronising the low pass filtered acceleration signal with the pulse signal are not the same length because of inaccuracies with the pulse signal. The signals are therefore resampled so that they can have exactly the same period. In this work the signals were resampled to 8192 sample points per gear rotation. There were 165 gear rotations per test. Synchronising the measured acceleration signal with the shaft encoder signal and resampling each signal to 8192 resulted in an input space of (165×8192). For convenience, in this work an input space of (160×8192) was selected. We seek to predict the time domain average (synchronous average) of the gear vibration using only a fraction of this input space.

In Chapter 3 it was shown that 40 rotation synchronised gear vibration signals are suitable for predicting TDA of the gear vibration signals. This result implies that an input space of dimensions (40×8192) can be used to calculate the TDA instead of the input space of (160×8192) that would otherwise be used when the direct time domain averaging approach is used to calculate the TDA. Using 40 rotation synchronised gear vibration signals instead of 160 rotation synchronised gear vibration signals is a reduction of 75 percent in the input data requirement. This result also has some implications in terms of the training and validation data sets. As stated above each test produces 165 rotation synchronised gear vibration signals. If 40 of the rotation synchronised gear vibration signals are used to train the neural network then the other 125 rotation synchronised gear vibration signals can be grouped in sets of 40 and used as validation sets. For this section of the work measurements were taken under constant load at different stages of gear life.

4.2.3 Model 1

In this section a model that utilises ANNs and SVMs to predict the TDA of gear vibration is presented. A sensitivity study to assess the sensitivity of the proposed model to number of inputs, number of hidden units, number of sample points per revolution and percentage noise in the validation sets is also presented. The training and validation data sets for Model 1 are tabulated in Table 4.3.

Table 4.3. Model 1 training and validation data sets for tests conducted under constant loading.

Gear life stage	**Test 1** New gear	**Test 2** Running in gear	**Test 3** Midlife	**Test 4** Advanced damage
Training set	1×(160×8192)	0	0	0
Validation sets	3×(160×8192)	4×(160×8192)	4×(160×8192)	4×(160×8192)

The first model (Model 1) utilises a simple feedforward network structure as shown in Figure 4.4. This model attempts to map the input space (rotation synchronised gear vibration signals) to the target (time domain average of the rotation synchronised gear vibration signal) using feedforward network structure in a single step.

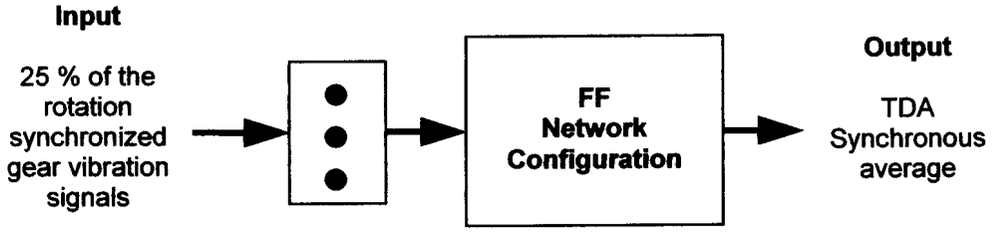

Figure 4.4 Model 1 with feedforward network structure.

Model 1 was investigated for all the formulations discussed in Chapter 3. The analysis of Model 1 with RBF and MLP was carried out in the following steps:

- The most suitable network architecture for mapping the input to the target is selected.

- The optimum number of inputs to the selected network architecture that correctly predicts the TDA of the gear vibration data using validation data sets are determined.
- The sensitivity of Model 1 with MLP or RBF networks to the number of sample points per revolution is assessed.
- A sensitivity study to assess the robustness of Model 1 with MLP or RBF networks with respect to noise is conducted.

4.2.3.1 Model 1 with MLP feedforward network

The first network formulation that was investigated is the MLP network. For convenience, the root mean square error given in Equation (4.1) was used to assess the performance of the neural network for the proposed model.

$$RMSE_k = \sqrt{\frac{1}{N_v}\sum_{i}^{N_v}\left(t_k^{(i)} - y_k^{(i)}\right)^2} \tag{4.1}$$

N_v is the number of validation data, $t_k^{(i)}$ is the target and $y_k^{(i)}$ is the network output. The optimum number of nodes and inputs were determined in order to correctly approximate the time domain averaging process while avoiding overfitting and thus bad generalisation.

A suitable network architecture was selected by first randomly choosing a network structure. The randomly selected structure was optimised sequentially by changing the network parameters while monitoring the *RMSE*, until a satisfactory time domain average prediction was obtained. The results obtained for analysis of the MLP using 20 unseen validation sets of dimensions (40×8192) are presented below. Figure 4.5 is a plot of *RMSE* against the number of hidden units.

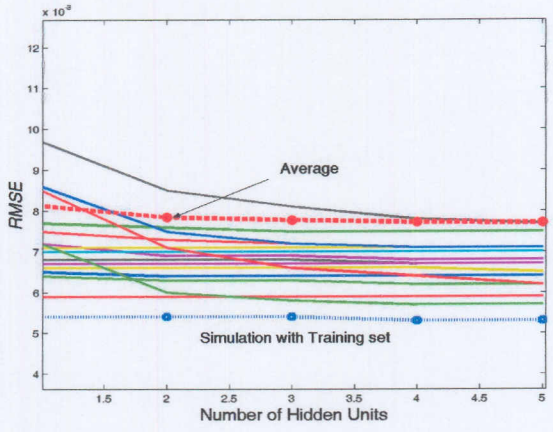

Figure 4.5 *RMSE* vs. Number of hidden units for 20 validation sets.

This plot shows that simulation with the training set is insensitive to the number of hidden units. When simulating with the validation sets there is general decrease in the *RMSE*, then it stabilises at four hidden units. This is because increasing the number of hidden units increases the flexibility of the network, thus increasing its capability to map the input to the output. This plot also shows the average of all the simulations with validation sets. The average shows insensitivity to the number of hidden units because most of the validation sets are fairly insensitive to the number of inputs. The average is somehow deceptive because some of the validation sets are sensitive to the number of inputs. The average can, however, still be useful for comparison purposes because the majority of the validation sets are insensitive to the number of hidden units. In this study an MLP network with 5 hidden units was selected. Figure 4.6 shows the *RMSE* plotted against the number of inputs for Model 1 simulated with 20 unseen validation sets.

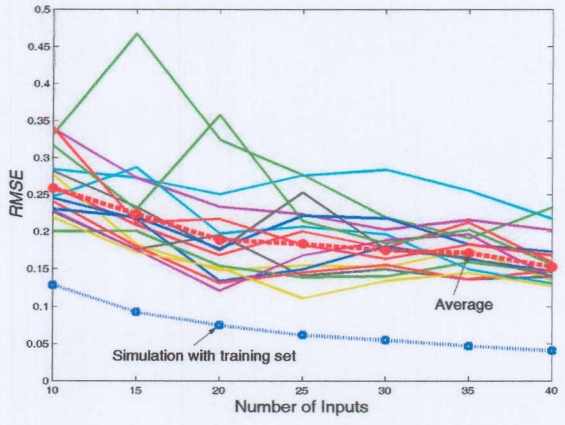

Figure 4.6 *RMSE* vs. Number of inputs for simulation with 20 validation sets.

Figure 4.6 shows the *RMSE* plotted against the number of inputs. In Chapter 3 it was established that 40 inputs were the optimal number of inputs for mapping the rotation synchronised gear vibration signals to the TDA, therefore, 40 inputs were selected as the maximum number of inputs in this analysis. In Figure 4.6 it is observed that the *RMSE* decreases as the number of inputs is increased. This is expected because the network is exposed to more of the underlying system dynamics, and therefore, trains and predicts more efficiently than would otherwise be the case with less inputs. The average of simulations with the validation sets and the simulation with the training set are also plotted. These plots also confirm the fact the as the network is exposed to more inputs, its prediction capabilities are enhanced. One of the objectives of this work is to decrease the number of inputs that are required to calculate the TDA, therefore, the analyst needs to make a compromise between the network accuracy and the number of inputs that are used. Figure 4.7 shows the *RMSE* plotted against the number of sample points per gear rotation.

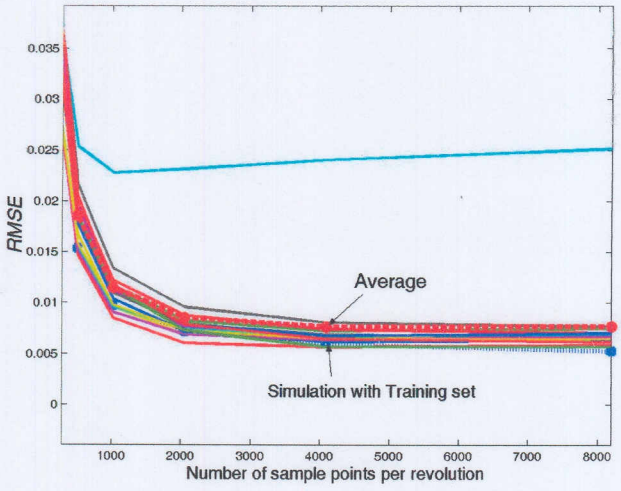

Figure 4.7 *RMSE* vs. number of sample points per revolution for 20 validation sets.

To assess the sensitivity to the number sample points per rotation synchronised gear vibration signal, the 20 validation sets with 40 inputs were resampled from 8192 sample points down to 4096, 2048, 1024, 512 and 256 respectively. Figure 4.7 shows the *RMSE* plotted against the number of sample points per revolution. The *RMSE* decreases until 2048 points per revolution, and thereafter remains constant. For the MLP simulation 1024 points per revolution were used to reduce computational load though 2048 sample points per revolution would have been more suitable. In Figure 4.7 it is

observed that there is a plot that is an outlier. This plot corresponds to the validation set that corresponds to the damaged gear. This is because vibration produced by the damaged gear is very different to that produced throughout the life of the gear, and the selected network did not generalise well to this condition. Figure 4.8 shows the *RMSE* plotted against percentage noise in the validation set.

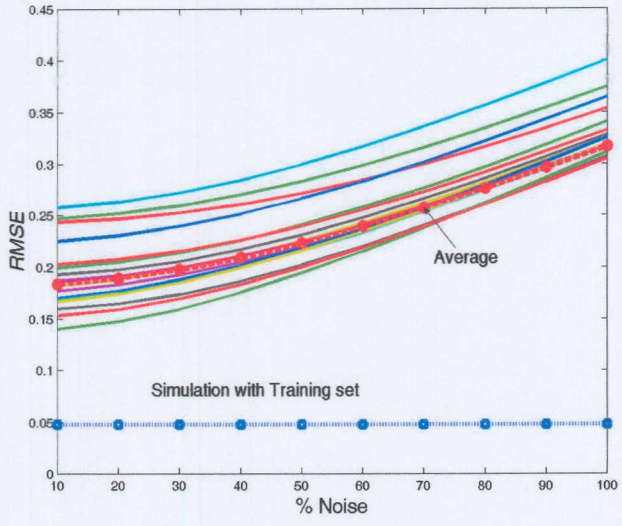

Figure 4.8 *RMSE* vs. percentage Noise in validation set for simulation with 20 validation sets.

Figure 4.8 shows the *RMSE* plotted against the percentage of random noise that is superimposed on the validation sets. The random noise is chosen from a normal distribution with a zero mean and variance of one. There is a direct relationship between the noise level and the *RMSE*. From this analysis Model 1 that has a MLP feedforward network was found to be fairly tolerant to noise.

4.2.3.2 Model 1 with RBF feedforward network

The second network formulation that was investigated for use in Model 1 is the RBF network. The procedure that was followed in the analysis of the MLP network was used for the RBF network. This section presents the results from the analysis of Model 1 with the RBF network. The sensitivity of Model 1 to number of inputs, number of hidden units, number of sample points per revolution and percentage noise superimposed on the validation sets is also presented. Figure 4.9 shows the *RMSE* plotted against number of hidden units (number of basis functions).

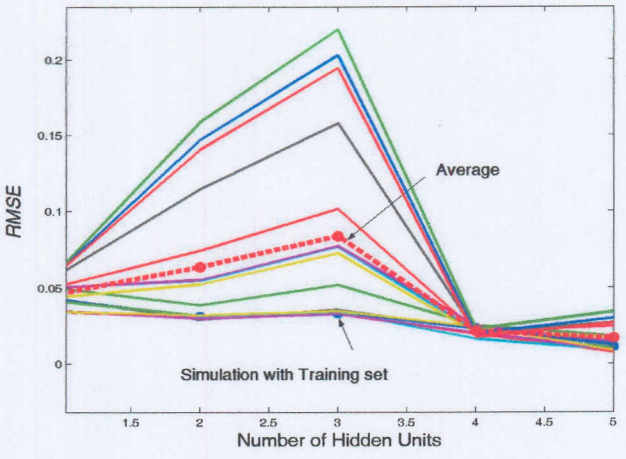

Figure 4.9 *RMSE* vs. number of hidden units for 20 validation sets.

Figure 4.9 shows the *RMSE* plotted against the number of hidden units (Number of basis functions). It is observed from this plot that the RBF is very sensitive to the number of basis functions. From Figure 4.9 it is observed that Model 1 with RBF network results in best generalisation at 4 basis functions, therefore 4 basis functions were selected for this study. It is possible that there is another optimum when more than 5 basis functions are used. To keep the computational load at a minimum it was decided to settle for 4 basis functions. Figure 4.10 shows the *RMSE* plotted against the number of inputs for Model 1 simulated with 20 unseen validation sets.

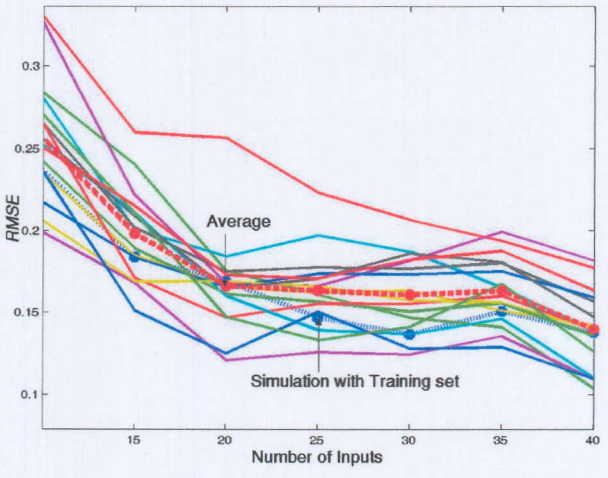

Figure 4.10 *RMSE* vs. number of inputs for simulation with 20 validation sets.

Figure 4.10 shows the *RMSE* plotted against the number of inputs. Again as observed for MLP network, the number *RMSE* decreases as the number of inputs is increased. For

RBF, there is a definite minimum for all the validation sets at 40 inputs. For this work 40 inputs were selected as the optimum number of inputs for Model 1 with RBF. Figure 4.11 shows the *RMSE* plotted against the number of sample points per gear rotation.

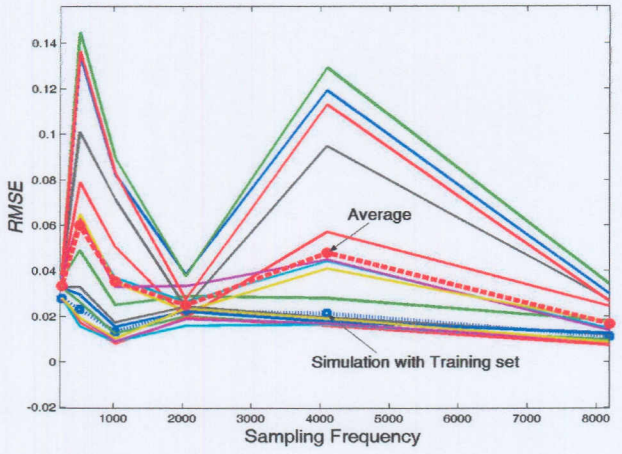

Figure 4.11 *RMSE* vs. number of sample points per revolution for 20 validation sets.

From this plot it is observed that the optimum number of sample points per revolution is 2048 but for computational efficiency 1024 points were selected. In Figure 4.12 the *RMSE* is plotted against the percentage noise in the validation set.

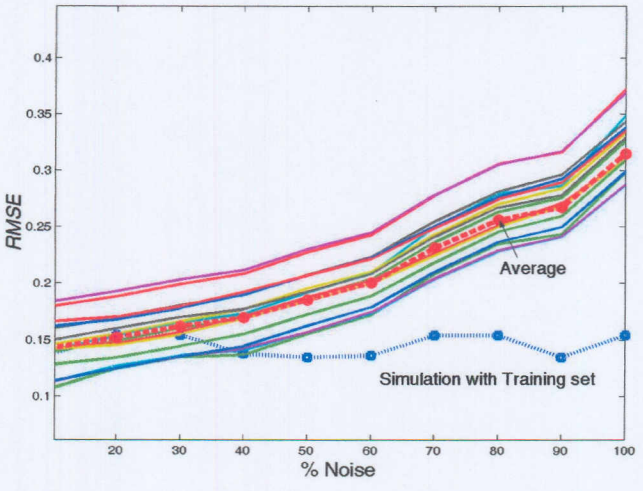

Figure 4.12 *RMSE* vs. percentage Noise in validation set for simulation with 20 validation sets.

Figure 4.12 is a plot of the *RMSE* against the percentage of random noise that is superimposed on the validation sets. There is again a direct relationship between the percentage noise and the *RMSE*. As the percentage noise increases so does the *RMSE*.

4.2.3.3 Model 1 with SVMs

This section presents the results from the analysis of Model 1 with SVMs. The sensitivity of Model 1 to number of inputs, number of hidden units, number of sample points per revolution and percentage noise superimposed on the validation sets is also presented.

The analysis of Model 1 with SVMs was carried out in the following steps:

- The most suitable Kernel function for mapping the input space to the target was selected.
- The optimum number of inputs for correctly predicting the TDA of the rotation synchronised gear vibration signals was determined.
- The sensitivity of Model 1 with SVMs to percentage noise in the validation sets was assessed.

Figure 4.13 shows the plot of the performance of different Kernel functions that were investigated in this study for the non-linear SVM regression task. In Figure 4.13 the *RMSE* produced by each of the Kernel function on an unseen validation set is plotted against the order of the Kernel function. From this plot, it is observed that the Exponential Radial Basis Function (ERBF) Kernel function outperforms the other Kernel functions. It is also observed that the ERBF Kernel function is insensitive to the order of the Kernel function. In this study the ERBF Kernel function with an order of 10 was therefore selected.

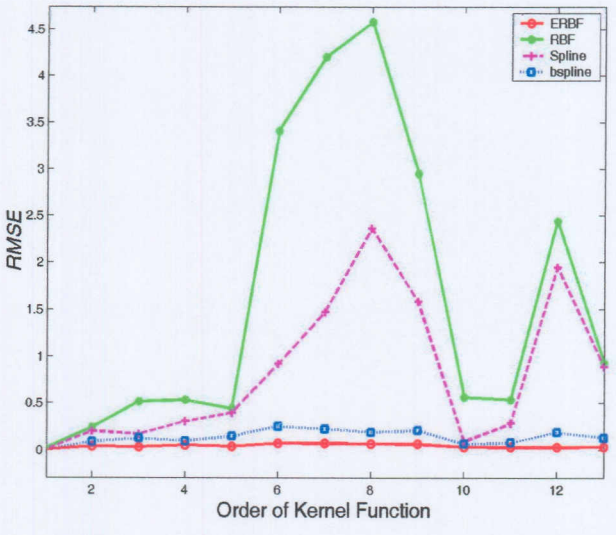

Figure 4.13 RMSE vs. Order of Kernel function an unseen validation sets.

Figure 4.14 shows the *RMSE* plotted against the number of inputs for Model 1 simulated with 20 unseen validation sets. It is observed from Figure 4.14 that simulation with the training set has a constant prediction error irrespective of the number of inputs. This is an indication of the robustness of the SVM algorithm. Simulation with validation sets indicates that there is an inverse proportionality between the number of inputs and the prediction error. This is because the SVM is exposed to more of the system dynamics as the number of inputs is increased; therefore, it trains more effectively.

SVMs are computationally expensive, therefore, in this work 256 points per rotation synchronised gear vibration signal were selected for all SVM analyses.

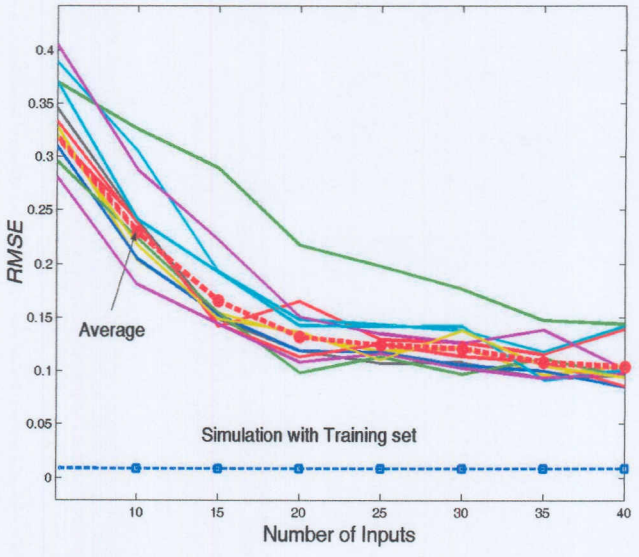

Figure 4.14 *RMSE* vs. number of inputs for 20 validation sets.

Figure 4.15 shows the *RMSE* plotted against percentage noise. A direct relationship between the *RMSE* and the percentage noise is observed. This is expected because the introduction of noise to the validation sets increases the degree of nonlinearity between the input and output space.

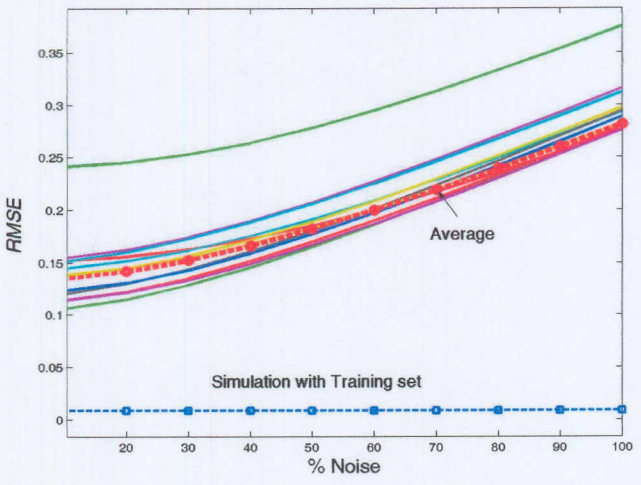

Figure 4.15 *RMSE* vs. percentage noise in validation set for simulation with 20 validation sets.

4.2.4 Model 2

In this section a second model (Model 2) that utilises ANNs and SVMs to predict TDA of gear vibration is presented. Model 2 estimates the TDA of the input space in small sequential steps, analogous to taking a running average of the input space. This model consists of a number of small feedforward networks similar to those in Model 1 but instead of the networks being used to predict the TDA of the whole input space in one step, the small feedforward networks are used to first sequentially predict the average of subsections of the input space (instantaneous averages). The output of the first set of feedforward networks are used as inputs into a second feedforward network that predicts the time domain average of the whole input space. All the feedforward networks are trained off-line to reduce computational time. In this model all the data that have already been used can be discarded immediately. This means that one does not need to store large amounts of data in the data collection system. The training and validation data sets for Model 2 are tabulated in Table 4.4.

Table 4.4. Model 2 training and validation data sets for tests conducted under constant loading.

Gear life stage	**Test 1** New gear	**Test 2** Running in gear	**Test 3** Midlife	**Test 4** Advanced damage
Training set	1×(10×8192)	0	0	0
Validation sets	15×(10×8192)	16×(10×8192)	16×(10×8192)	16×(10×8192)

In this section a sensitivity study to assess the sensitivity of the proposed model to number of inputs, number of hidden units, number of sample points per revolution and percentage noise in the validation sets is presented. A schematic diagram of Model 2 is shown in Figure 4.16.

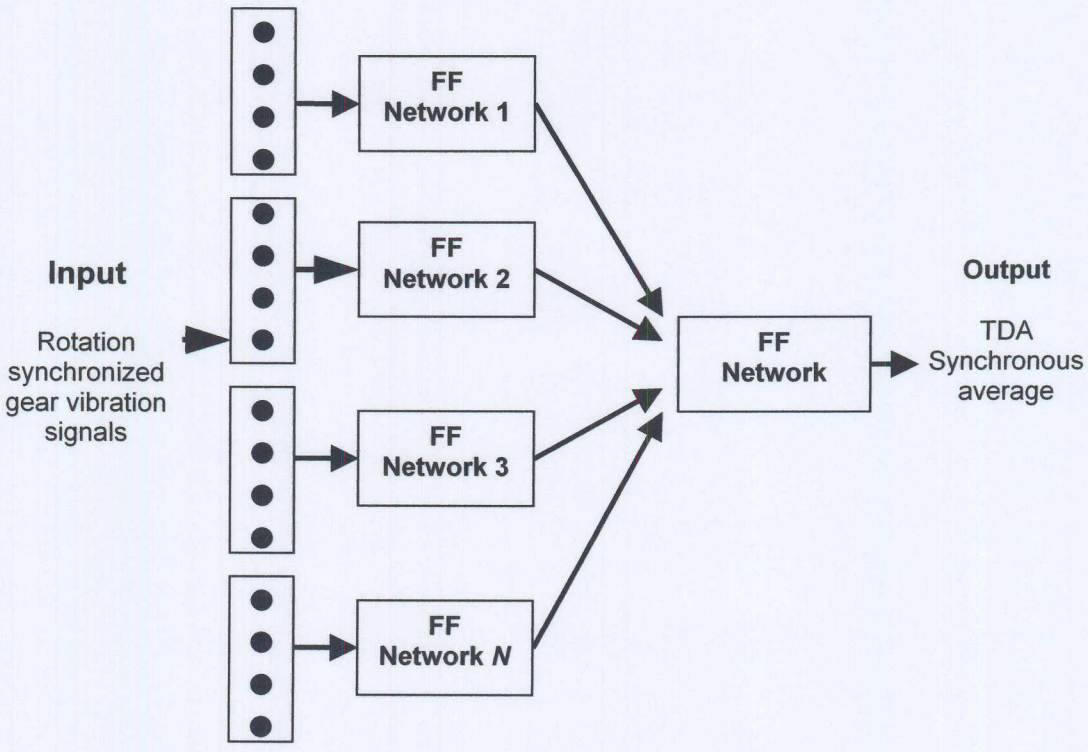

Figure 4.16 Model 2

Model 2 was investigated for all the formulations discussed in Chapter 3. The analysis of Model 2 with RBF and MLP was carried out in the following steps:

- The most suitable network architecture for mapping a small section of the input to its average (target) is selected.
- The sensitivity of Model 2 with MLP or RBF networks to noise is assessed.
- In Section 4.2.3.1 and Section 4.2.3.1 the sensitivity of Model 1 with MLP and RBF networks to the number of sample points per rotation synchronised gear vibration was assessed. It was concluded the 1024 points per revolution are suitable, therefore 1024 sample points per rotation synchronised gear vibration signal are selected for Model 2.

4.2.4.1 Model 2 with MLP feedforward networks

This section presents the results from the analysis of Model 2 with MLP feedforward networks. Figure 4.17 shows the simulation results of Model 2 with MLP network simulated using an unseen validation set. The simulation result is superimposed on TDA calculated using the direct time domain averaging approach.

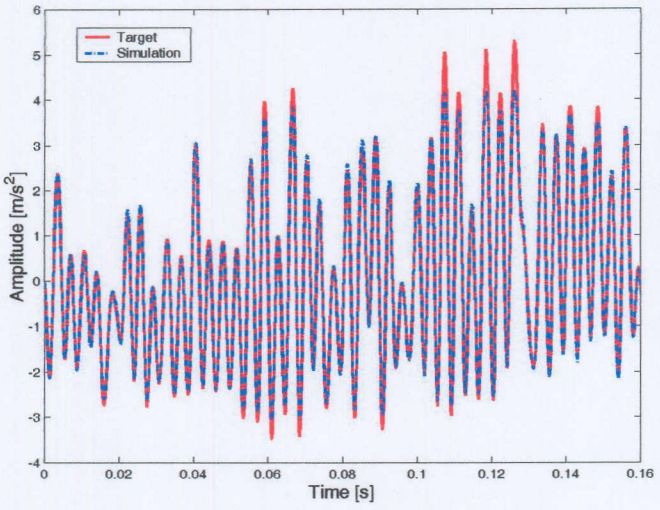

Figure 4.17 Model 2 with MLP network simulation result for an unseen validation set superimposed on TDA after 160 gear rotations.

This plot shows that Model 2 with MLP feedforward networks is very suitable for predicting the time domain average of the gear vibration. This is because Model 2 uses the whole input space to predict the TDA as opposed to Model 1 that uses only a section of the input space. Figure 4.18 shows the *RMSE* plotted against percentage noise in the training and validation sets. The random noise content is again chosen from a normal distribution with a zero mean and variance of one. For the simulation with the training set it is observed that the model is fairly insensitive to noise. This is, however, not the case when simulating with validation sets. There is a direct relationship between the *RMSE* and the percentage noise superimposed in the data. This is because addition of noise to the training and validation sets increases the degree of non-linearity between the input space and the output.

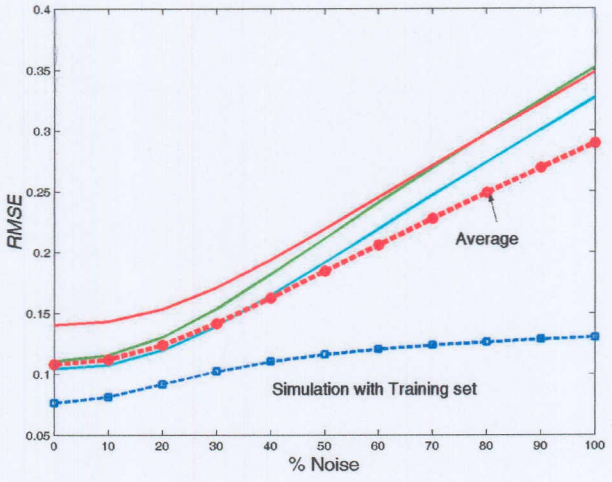

Figure 4.18 *RMSE* vs. percentage noise in training and validation sets for 3 unseen validation sets.

4.2.4.2 Model 2 with RBF feedforward networks

This section presents the results from the analysis of Model 2 with RBF feedforward network. In Figure 4.19 the simulation results of Model 2 with RBF network simulated using an unseen validation set is superimposed on the TDA calculated using direct averaging. The predicted TDA in Figure 4.19 is almost an exact fit. This is because Model 2 uses the whole input space to predict the TDA; therefore the network is exposed to all the transient effects in the data.

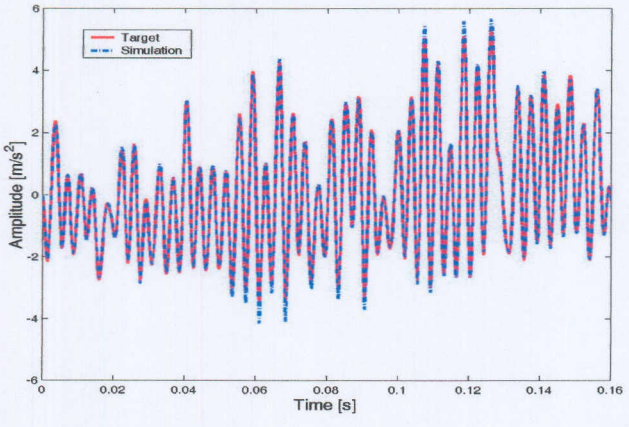

Figure 4.19 Model 2 with RBF network simulation result for an unseen validation set superimposed on TDA after 160 gear rotations

Figure 4.20 shows the *RMSE* from 3 validation sets plotted against percentage noise in the training and the validation sets. Both the training and the validation sets exhibit a linear relationship between the *RMSE* and the percentage noise superimposed in the

data. This is again because addition of noise to the training and validation sets increases the degree of non-linearity between the input space and the output.

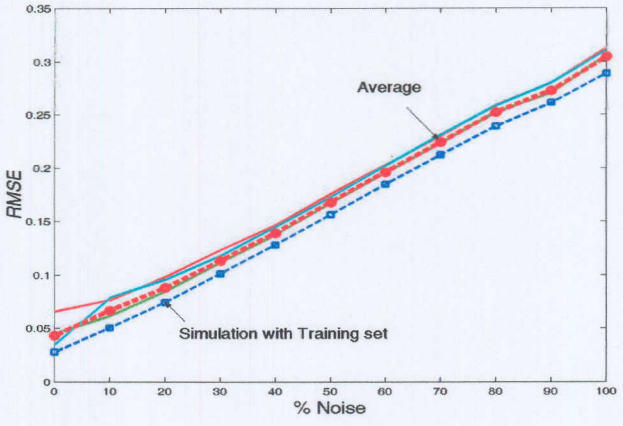

Figure 4.20 *RMSE* vs. percentage noise in training and validation sets for 3 unseen validation sets.

4.2.3.3 Model 2 with SVMs

This section presents the results from the analysis of Model 2 with SVMs in place of feedforward neural networks. Figure 4.21 shows that the SVM is also suitable for use in this modal with its only drawback being computational inefficiency. The good performance of Model 2 is because it uses the whole input space to predict the TDA; therefore the SVM is exposed to all the transient effects in the data. To maintain the computation time at a minimum, 256 samples points per rotation synchronised gear vibration signal were selected.

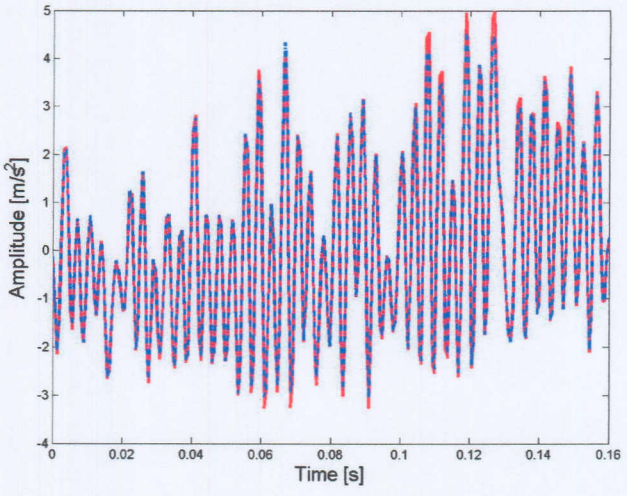

Figure 4.21 Model 2 with SVM simulation results with an unseen validation set superimposed on TDA after 160 gear rotations

Figure 4.22 shows the *RMSE* from 3 validation sets plotted against percentage noise in the training and the validation sets. With SVM the simulation with training set shows that the support vector machine is fairly insensitive to noise. This is not the case when simulating with the validation sets. Simulations with the validation sets indicate a direct relationship between the *RMSE* and the percentage noise in the data. The observed direct relationship is due to the fact that the addition of noise to the training and validation sets increases the degree of non-linearity between the input space and the output.

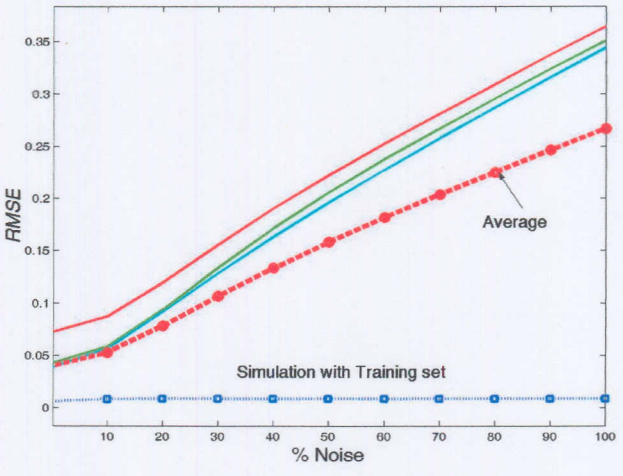

Figure 4.22 *RMSE* vs. percentage Noise in training and validation sets for 3 unseen validation sets.

4.2.5 Discussion

In this section a comparison between the different mathematical formulations is presented. The comparison is based on the average *RMSE* of simulation with a population of 20 validation sets (validation examples) for Model 1 and 3 validation sets (validation examples) for Model 2 an computation time.

4.2.5.1 Model 1

Figure 4.23 to Figure 4.26 show the results obtained for different formulations as functions of some network parameters. Figure 4.23 shows the *RMSE* plotted against the number of hidden units. From this plot it is observed that the MLP network performs better than the RBF network. The RBF network is very sensitive to the number of hidden units while the MLP is fairly insensitive. The insensitivity of MLP to the number of hidden units is desirable because it implies that smaller and more computationally

of hidden units is desirable because it implies that smaller and more computationally efficient networks can be used to calculate the TDA. Figure 4.24 shows the *RMSE* plotted against the number of inputs for Model 1 with MLP, RBF networks and SVM respectively. From this plot is observed that Model 1 with SVMs results in the best performance especially at higher number of inputs. The superior performance is because of the structural risk minimisation used in SVMs is superior in generalisation to the empirical risk minimisation used in neural network (Gunn et al., 1998). The performance of Model 1 with RBF and MLP networks are comparable although the RBF performs slightly better than MLP.

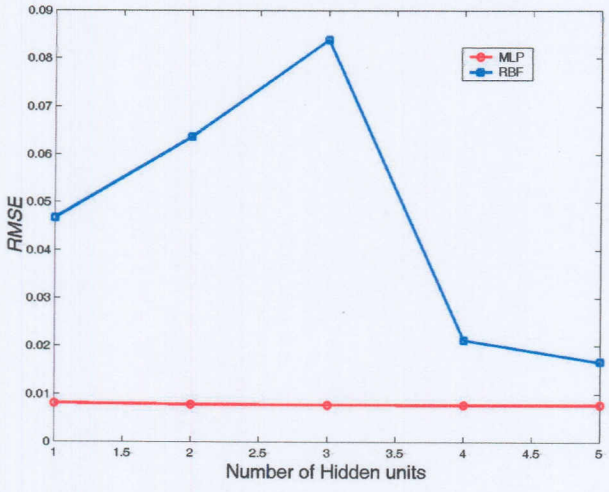

Figure 4.23 *RMSE* vs. number of hidden units for Model 1 with MLP and RBF networks.

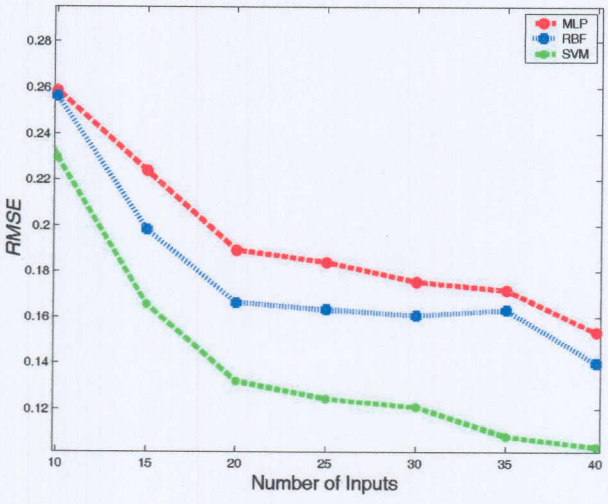

Figure 4.24 *RMSE* vs. number of inputs for Model 1 with MLP, RBF and SVMs.

In Figure 4.24 the reduction in *RMSE* as the number of inputs is increased is because the formulations are exposed to more of the underlying system dynamics as the number of inputs is increased, therefore they train more efficiently. Figure 4.25 shows *RMSE* plotted against the number of sample points per revolution. This plot shows that Model 1 with MLP network performs better than Model 1 with RBF network, which is very sensitive to the number of sample points per revolution. Figure 4.26 shows the performance of the three formulations as a function of percentage noise in the training and validation sets. This plot shows that the SVM again performs better than both MLP and RBF although the performances are fairly comparable. This is due to the superior performance of the structural risk minimisation used in SVMs (Vapnik, 1995; Gunn, 1998).

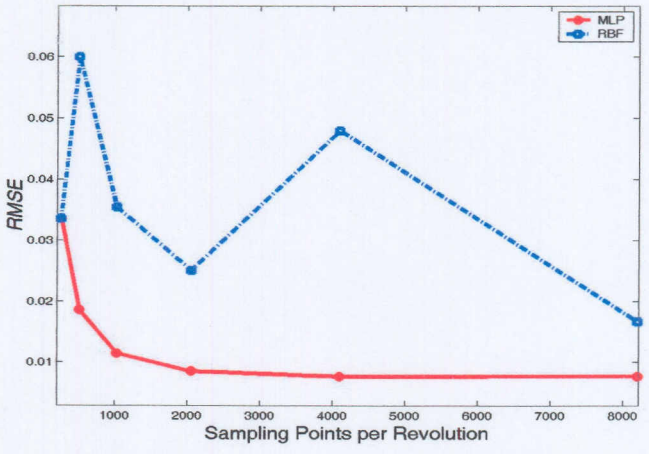

Figure 4.25 *RMSE* vs. number of sample points per revolution for Model 1 with MLP and RBF networks.

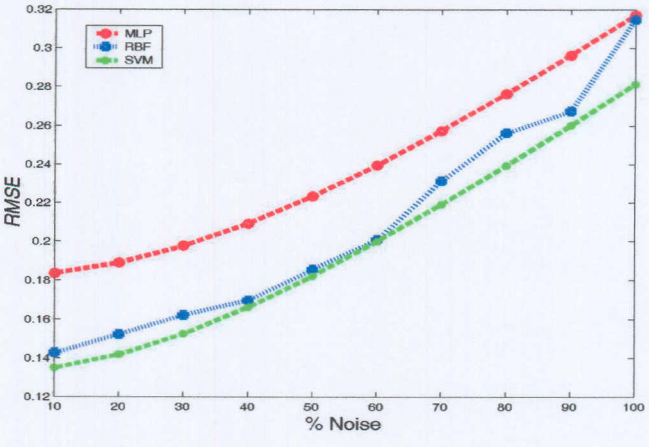

Figure 4.26 *RMSE* vs. percentage noise in training and validation sets for Model 1 with MLP, RBF and SVMs.

4.2.5.2 Model 2

Figure 4.27 and Figure 4.28 show the performance of Model 2 with the three formulations. Figure 4.27 shows the *RMSE* produced by 3 different validation sets. The SVM performs very well when simulating with the training set but performs poorly for validation sets. MLP and RBF both perform better than the SVMs for the validation sets. The poorer performance of Model 2 with SVM as compared to Model 2 with MLP and RBF networks is due to the fact that MLP and RBF are more suited to Model 2.

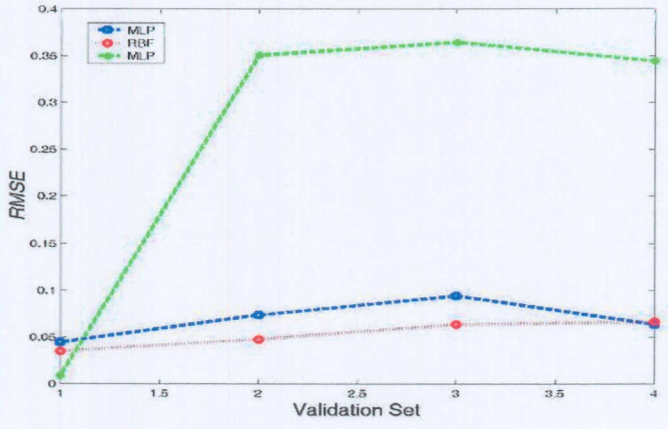

Figure 4.27 *RMSE* vs. validation set for 3 validation sets

Figure 4.28 shows the performance Model 2 with MLP, RBF and SVMs as a function of the percentage noise in the training and validation sets. It is observed that the performance of these formulations is the same. The observed direct relationship between the percentage noise in the training and validation sets and the *RMSE* is because the addition of noise increases the degree of non-linearity between the input space and the output.

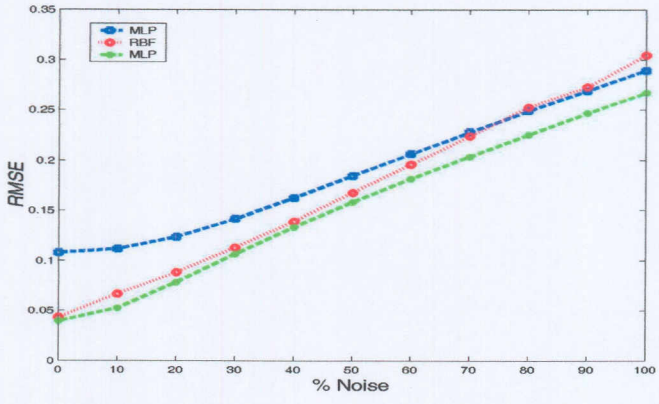

Figure 4.28 *RMSE* vs. percentage noise in training and validation sets for Model 2 with MLP, RBF and SVMs.

4.2.5.3 Computation time

To put the proposed methods in perspective, a comparison of computation times for the existing time domain averaging method and the proposed models is done. A Pentium 4 computer with a 1.60 GHz processor was used. The computation times are presented in Table 4.5.

It is observed that the required pre-processing time for Model 1 is less than the required pre-processing time for the TDA calculated by direct averaging. This is because Model 1 uses 25 percent of the vibration data as opposed to the original TDA process, which uses the all the vibration data. The required pre-processing time for Model 2 is equal to the pre-processing time for the TDA calculated by direct averaging. This is because both models use the same amount of vibration data. When Model 1 and Model 2 are used, RBF and MLP give the best performance in terms of simulating time and SVMs gives the poorest performance. The models are trained off-line therefore the training time does not influence the simulating time in a real time applications. When the models are used with MLP and RBF networks, they perform much better than original TDA calculated by direct averaging in terms of simulation time. It is however, observed that when the models are used with SVMs, the performance is much poorer than the performance of the TDA computed by direct averaging.

The poor performance in SVMs is because the training problem is a quadratic optimisation problem with 2N variables, where N is the number of data training points. Thus the more the data that is used when train, the longer it takes. This is much slower than the MLP and RBF neural networks in which only the weights and biases or the basis centres are obtained by minimising error functions.

Table 4.5 Computation time

	TDA	**MLP**	**RBF**	**SVM**
Model 1 Pre-processing time [s]	1.011	0.703	0.703	0.703
Model 1 Training time [s]	-	22.24	2.219	497.0
Model 1 simulating time [s]	0.75	0.016	0.047	5.500
Model 2 Pre-processing time [s]	1.011	1.011	1.011	1.011
Model 2 Training time [s]	-	1.14	1.015	963.8
Model 2 simulating time[s]	-	0.08	0.078	83.76

4.3 Conclusion

In this chapter the use of MLP, RBF neural networks and SVMs in the development of a time domain averaging filter for gear vibration was investigated. It was shown that the amount of input vibration data required to calculate the TDA can be effectively reduced using ANNs and SVMs to predict the TDA of a gear vibration signal.

Two different filter models are considered. The first model (Model 1) uses a feedforward ANNs or SVMs to map input space (rotations synchronised gear vibration signals) to the target (time domain average after 160 shaft rotations). Using Model 1 a data reduction of 75 percent was achieved with all the formulations because Model 1 predicted the TDA using 40 of the 160 rotation synchronised gear vibration signals. Any of the three formulations can be used in this model because their performances are comparable although the SVMs may seem to be more attractive. Its attractiveness is reduced by the fact that it is more computationally expensive than MLP and RBF, therefore, the analyst will need to be cautious when SVMs are implemented in an online system that is required to retrain regularly. On the other hand the MLP and RBF networks are quick and easy to train, therefore they are suitable for implementation in an online system even when required to retrain online.

The second model (Model 2) operates in two stages. In the first stage it uses 10 inputs (10 rotations synchronised gear vibration signals) to predict the instantaneous time domain average of the gear vibration. The input data to the first stage is deleted from the memory of the data acquisition system after it has been used. The output of the first stage is used as input to a second feedfoward network to predict the TDA. This means that the largest number of rotation synchronised gear vibration signals that will be stored in the data acquisition system is 26 inputs. This is a reduction of 83 percent in the amount of data that needs to be stored in the data acquisition system. It must be noted however that, with Model 2, the entire data set is used although it use sequentially. Model 2 was found to be very effective at predicting the time domain average for all three formulations. In Model 2 the MLP and RBF perform better than SVMs.